

# Electronic structure and spontaneous internal field around non-magnetic impurities in spin-triplet chiral $p$ -wave superconductors

Mitsuaki Takigawa\*

*Department of Computational Science and Engineering,  
21st century COE, Nagoya University, Nagoya 464-8601, Japan*

Masanori Ichioka

*Department of Physics, Okayama University, Okayama 700-8530, Japan*

Kazuhiko Kuroki

*Department of Applied Physics and Chemistry, the University of Electro-Communications, Chofu, Tokyo 182-8585, Japan*

Yukio Tanaka

*Department of Material Science and Technology, Nagoya University, Nagoya 464-8603, Japan*

(Dated: November 14, 2018)

The electronic structure around an impurity in spin triplet  $p$ -wave superconductors is studied by the Bogoliubov-de Gennes theory on a tight-binding model, where we have chosen  $\sin p_x + i \sin p_y$ -wave or  $\sin(p_x + p_y) + i \sin(-p_x + p_y)$ -wave states which are considered to be candidates for the pairing state in  $\text{Sr}_2\text{RuO}_4$ . We calculate the spontaneous current and the local density of states around the impurity and discuss the difference between the two types of pairing. We propose that it is possible to discriminate the two pairing states by studying the spatial dependence of the magnetic field around a pair of impurities.

PACS numbers: 74.25.Jb, 74.20.Rp, 73.20.Hb, 74.70.Pq

The discovery of superconductivity in  $\text{Sr}_2\text{RuO}_4$  by Maeno *et al.* [1] has highly activated the field of spin-triplet superconductivity[2]. There are several key evidences suggesting that spin-triplet pairing is realized in  $\text{Sr}_2\text{RuO}_4$  [3, 4, 5, 6, 7, 8, 9]. The presence of spontaneous magnetic field suggested from  $\mu\text{SR}$  experiment is consistent with a chiral superconductivity with broken time reversal symmetry (BTRSS) [10]. Tunneling spectroscopy with zero bias conductance peak [11] is also consistent with spin-triplet pairing with BTRSS [12].

Theoretically, several pairing states and/or microscopic mechanisms for spin-triplet  $p$ -wave pairing have been proposed [13, 14, 15, 16, 17]. Although there are three bands in  $\text{Sr}_2\text{RuO}_4$ , it is possible to consider the essence of the superconducting property only by considering quasi two-dimensional  $\gamma$ -band. For simplicity, here we classify the pairings for  $\text{Sr}_2\text{RuO}_4$  into two types, which are qualitatively consistent with experiments of specific heat.[18] The first type is  $\sin p_x + i \sin p_y$ -wave proposed by Miyake and Narikiyo (MN), where cooper pairs are formed between nearest neighbor sites. The second one is  $\sin(p_x + p_y) + i \sin(-p_x + p_y)$ -wave state proposed by Arita, Onari, Kuroki, and Aoki (AOKA)[15], where pairs are formed between next nearest neighbor sites. The pairing which has been proposed based on third order perturbation theory [16, 17] has more higher harmonics where the most dominant component is  $\sin(p_x + p_y) + i \sin(-p_x + p_y)$ -wave pairing.

In the following, we call  $\sin p_x + i \sin p_y$ -wave pairing and  $\sin(p_x + p_y) + i \sin(-p_x + p_y)$ -wave pairing as MN-type pairing and AOKA-type, respectively. The discrimination between the MN-type and the AOKA-type pairings is important because it is strongly related to the study of the superconducting properties and the pairing mechanism of  $\text{Sr}_2\text{RuO}_4$ . One of the remarkable difference of the two pairing states is the winding number of the pairing function when we trace its phase along the  $\gamma$ -band Fermi surface [19]. The winding number is one in the MN-type pairing, but three in the AOKA-type pairing. It is interesting to propose a new idea to discriminate these two pairings having different topological characters.

The aim of the present paper is to propose that experimental observation of the electronic properties and the internal field around the impurity can be used to discriminate the two pairing states. Actually, as shown in recent experiments by Lupien *et al.*, it is possible to observe the local density states in  $\text{Sr}_2\text{RuO}_4$  with high accuracy [20]. It is shown in the previous studies that the electronic structure is modulated around the impurity [21, 22, 23]. For superconductors with BTRSS, circular current is induced around impurities [24] and a spontaneous field appears by a non-magnetic impurity. In this paper, we calculate the local density of states (LDOS) and spontaneous internal field around the non-magnetic impurity, and discuss the difference between the two pairings.

To obtain the wave functions and the eigenenergies around the impurity, we solve the Bogoliubov-de Gennes (BdG) equation on a tight binding model which takes into account the anisotropy of the Fermi surface and the

---

\*Electronic address: takigawa@fcs.coe.nagoya-u.ac.jp

superconducting gap structure [19],

$$\sum_i \begin{pmatrix} K_{ji} & \Delta_{ij} \\ \Delta_{ij}^\dagger & -K_{ji}^* \end{pmatrix} \begin{pmatrix} u_\epsilon(\mathbf{r}_i) \\ v_\epsilon(\mathbf{r}_i) \end{pmatrix} = E_\epsilon \begin{pmatrix} u_\epsilon(\mathbf{r}_j) \\ v_\epsilon(\mathbf{r}_j) \end{pmatrix}, \quad (1)$$

where  $K_{i,j} = -t_{i,j} - \mu\delta_{i,j}$  and  $\epsilon$  is an index of the eigenstates. We set  $t_{i,j} = t$ ,  $(-0.4t)$  for the transfer between nearest (second nearest) neighbor sites in the two dimensional square lattice of Ru atoms, and the chemical potential  $\mu$  which depends on the temperature is tuned so that the density of electron is fixed at  $\langle n \rangle = 4/3$ . This reproduces the Fermi surface topology of the  $\gamma$ -sheet in  $\text{Sr}_2\text{RuO}_4$ . The energy and the temperature are scaled by  $t$  throughout this paper. The self-consistent condition is

$$\Delta_{ij} = g_{z,ji}(\langle a_{j\downarrow}a_{i\uparrow} \rangle + \langle a_{j\uparrow}a_{i\downarrow} \rangle) \quad (2)$$

with  $\langle a_{j\downarrow}a_{i\uparrow} \rangle = \sum_\epsilon v_\epsilon^*(\mathbf{r}_j)u_\epsilon(\mathbf{r}_i)f(E_\epsilon)$  and  $\langle a_{j\uparrow}a_{i\downarrow} \rangle = \sum_\epsilon u_\epsilon(\mathbf{r}_j)v_\epsilon^*(\mathbf{r}_i)f(-E_\epsilon)$ , where  $f(E)$  is the Fermi distribution function, and  $g_{z,ji}$  is the spin triplet pairing interaction.

The orbital part of the pair potential at each site  $i$  can be decomposed into  $\sin p_x$ - and  $\sin p_y$ -components as

$$\Delta_{p_x}(\mathbf{r}_i) = (\Delta_{i,i+\hat{x}} - \Delta_{i,i-\hat{x}})/2, \quad (3)$$

$$\Delta_{p_y}(\mathbf{r}_i) = (\Delta_{i,i+\hat{y}} - \Delta_{i,i-\hat{y}})/2 \quad (4)$$

as  $g_{z,ij}$  is non-zero only for nearest neighbor (NN) site pair in the MN-type pairing. For  $\sin p_x \pm i \sin p_y$ -wave superconductivity, we define the pair potential as  $\Delta_\pm(\mathbf{r}_i) \equiv \Delta_{p_x}(\mathbf{r}_i) \pm i \Delta_{p_y}(\mathbf{r}_i)$ . When the pair potential is uniform, this BdG formulation is reduced to the conventional theory for  $p$ -wave superconductors with the MN-type pairing functions, which has an anisotropic gap  $(\sin^2 p_x + \sin^2 p_y)^{1/2}$ . In the AOKA-type pairing case, as  $g_{z,ij}$  is non-zero only for second nearest site pairs, the pair potential  $\Delta'_\pm(\mathbf{r}_i)$  is defined by  $\Delta_{i,i+(\hat{x}+\hat{y})}$  and  $\Delta_{i,i+(-\hat{x}+\hat{y})}$  instead of  $\Delta_{i,i+\hat{x}}$  and  $\Delta_{i,i+\hat{y}}$ .

To investigate the electronic structure around the impurity, we calculate the LDOS at the  $i$ -th site as

$$N(E, \mathbf{r}_i) = \sum_\epsilon \{ |u_\epsilon(\mathbf{r}_i)|^2 \delta(E - E_\epsilon) + |v_\epsilon(\mathbf{r}_i)|^2 \delta(E + E_\epsilon) \}. \quad (5)$$

We evaluate the spontaneous internal field  $\mathbf{H}(\mathbf{r})$  through the Maxwell equation:  $\nabla \times \mathbf{H} = \frac{4\pi}{c} \mathbf{j}(\mathbf{r})$ . The current  $\mathbf{j}(\mathbf{r})$  is calculated as

$$\begin{aligned} j_{\hat{e}}(\mathbf{r}_i) &= 2|e|c \text{Im} \{ \tilde{t}_{i+\hat{e},i} \sum_\sigma \langle a_{i+\hat{e},\sigma}^\dagger a_{i,\sigma} \rangle \} \\ &= 2|e|c \text{Im} \{ \tilde{t}_{i+\hat{e},i} \sum_\alpha [u_\alpha^*(\mathbf{r}_{i+\hat{e}})u_\alpha(\mathbf{r}_i)f(E_\alpha) \\ &\quad + v_\alpha(\mathbf{r}_{i+\hat{e}})v_\alpha^*(\mathbf{r}_i)(1-f(E_\alpha))] \} \end{aligned} \quad (6)$$

for the  $\hat{e}$ -direction bond ( $\hat{e} = \pm\hat{x}, \pm\hat{y}$ ) at site  $\mathbf{r}_i$ . The spontaneous current  $j_{\hat{e}}(\mathbf{r}_i)$  circles around the impurity when time reversal symmetry is broken.

We consider a system with a square unit cell of  $N_r \times N_r$  sites where an impurity is located at the center of the

unit cell. By introducing the quasi-momentum of the Bloch state, we obtain the wave function under the periodic boundary condition whose region covers  $N_k \times N_k$  unit cells. We typically consider the case  $N_r=31$  and  $g_{z,ji} = -t$  at a low temperature  $T = 0.01t$ . The chemical potential at the impurity site is taken as  $\mu_{\text{imp}} = -16.0t$ . The wave function is almost zero at the impurity site.

First, we study the properties around a single impurity, and compare the results between the MN-type and the AOKA-type pairing cases. Figure 1 shows the pair potential structure around the impurity for MN-type pairing and for AOKA-type pairing. The amplitude of the dominant chiral component ( $\Delta_+$  or  $\Delta'_+$  here) vanishes at the impurity site, and recovers within a few site from the impurity, as shown in Fig. 1(a). On the other hand, the other component with opposite chirality ( $\Delta_-$  or  $\Delta'_-$ ) is induced around the impurity as shown in Fig. 1(b). The phase structure of the induced component, shown in Fig. 1(c), has a remarkable difference between the two pairing cases, reflecting the winding along the Fermi surface. In the MN case,  $\text{Arg}\Delta_-$  has +2-winding at the impurity site, and -1-winding at four sites located eight sites away from the impurity along the vertical and the horizontal directions. In the AOKA case,  $\text{Arg}\Delta'_-$  has -6-winding at the impurity site, and +1-windings at four sites located on the diagonal directions in addition to +1-windings at four sites on the vertical and horizontal directions. Since the amplitude of the induced component vanishes at these winding center sites,  $|\Delta'_+|$  is more suppressed around the impurity with -6-winding, and the tails of  $|\Delta'_+|$  have a shape extending toward eight directions far from the impurity. For the difference of the winding structure of the induced chiral component, there appears some differences between the MN-type and the AOKA-type pairings in the structure around impurities.

In Fig. 2(a), we plot the spontaneous current  $j_{\hat{e}}(\mathbf{r})$  around the impurity. The current circles around the impurity, and the staggered current spreads toward the diagonal directions. The current in the diagonal direction is larger in the MN case. We show the internal magnetic field in Fig. 2(b). The spontaneous field at the impurity site is oriented to the  $-z$  direction. This induced field is larger in the AOKA case, since the the spontaneous current around the impurity is larger [Fig. 2(a)] due to the -6-winding of  $\Delta'_-$  at the impurity [Fig. 1(c)]. To compensate the spontaneous field at the impurity site, the spontaneous field is oriented toward the  $+z$  direction near the impurity along the horizontal and vertical directions.

Figure 3(a) shows the LDOS  $N(E, \mathbf{r}_i)$  around the impurity. The impurity is located at site (16,16). We plot the  $N(E, \mathbf{r}_i)$  at the nearest site  $\mathbf{r}_i = (15, 16)$ , at the second nearest site (15,15), and at the farthest site (1,1). The energy spectrum of the uniform state with  $p$ -wave anisotropic gap is reproduced at (1,1). Splitted LDOS peaks appear within the gap at (15,15) and (15,16) near the impurity. The side peak in the positive energy range is larger than that in the negative range for both pair-

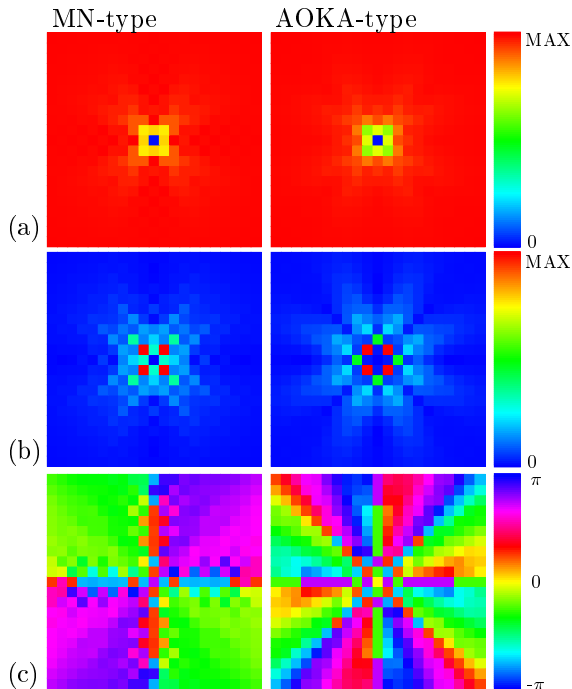


FIG. 1: (Color) Spatial structure of the pairing potential for the MN-type (left panels) and the AOKA-type (right panels) pairings. We shown a region consisting of  $21 \times 21$  sites with the impurity located at the center. (a) Amplitude of the dominant chiral component,  $|\Delta_+(\mathbf{r})|$  or  $|\Delta'_+(\mathbf{r})|$ . (b) Amplitude of the induced opposite chiral component,  $|\Delta_-(\mathbf{r})|$  or  $|\Delta'_-(\mathbf{r})|$ . (c) Phase structure of the the induced component,  $\text{Arg}\Delta_-(\mathbf{r})$  or  $\text{Arg}\Delta'_-(\mathbf{r})$ . The phase of the dominant chiral component is almost uniform.

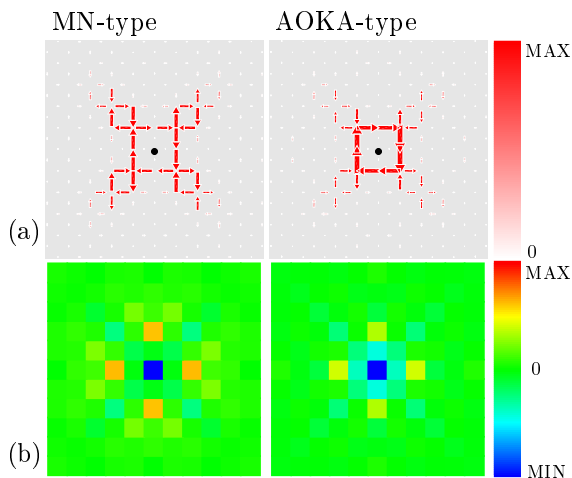


FIG. 2: (Color) The spontaneous current  $j_e(\mathbf{r})$  (a) and the internal magnetic field distribution  $H(\mathbf{r})$  (b) around a single impurity for the MN-type (left panels) and the AOKA-type (right panels) pairings. We show a region consisting of  $11 \times 11$  sites with the impurity at the center. Solid circles in (a) indicate the impurity site.

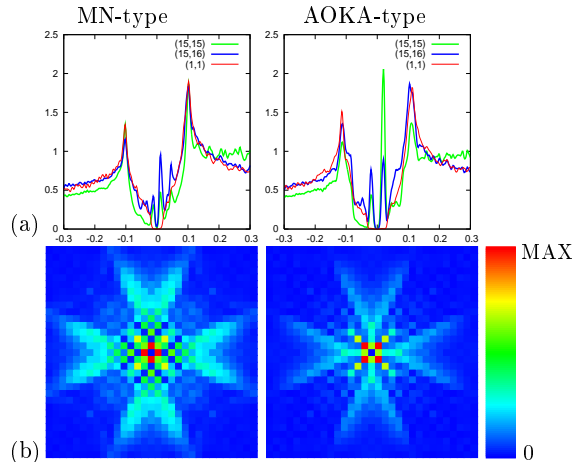


FIG. 3: (Color) (a) Spectrum of the LDOS  $N(E, \mathbf{r})$  at sites (15,15), (15,16) and (1,1). (b) Density plot of the LDOS  $N(E \sim 0, \mathbf{r})$  at the peak energy of the spectrum near  $E \sim 0$  within a unit cell of  $31 \times 31$  sites. The left and right panels are, respectively, for the MN-type and the AOKA-type pairings.

ings. The peak at (15,15) is larger (smaller) than that at (15,16) in AOKA-type (MN-type) pairing. The LDOS at this peak energy is shown in Fig. 3(b). The tail structure far from the impurity is similar, but the LDOS at nearest and second nearest sites is different between MN-type and AOKA-type pairings. In the case of AOKA-type (MN-type) pairing between diagonal (vertical) site quasiparticles, the low energy state is likely to appear in the diagonal (vertical) site next to the impurity site. The anisotropic gap structure on the Fermi surface also contributes to the difference of the LDOS. In the AOKA-type pairing, the gap amplitude has local minimum at  $[110]$  directions on the Fermi surface in addition to the minimum at  $[100]$  directions, as shown in Fig. 1 of ref. [19].

As we have seen in Fig. 2(b), a drastic qualitative difference is not seen in the internal field between the two pairings in the case of single impurity. However, in multiple impurity case, there are some cases producing qualitative differences between the two pairing cases in the spontaneous field distribution around the impurities due to the interference of the phase of the induced opposite chiral component (i.e.  $\Delta_-(\mathbf{r})$  or  $\Delta'_-(\mathbf{r})$  in Fig. 1). As an example of this effect, we report the case when two impurities are located at next nearest neighboring sites, i.e., sites (15,15) and (16,16) in our calculation. As in the single impurity case, the zero energy LDOS is large at the nearest site of the impurities for MN-type, and at the next nearest site for AOKA-type. As shown in Fig. 4, the spontaneous current and the field distribution is not a simple summation of the distribution of the single impurity case, since the strong interference is at work between the two impurities. It is remarkable that for MN-type pairing, the field intensity is strong in the

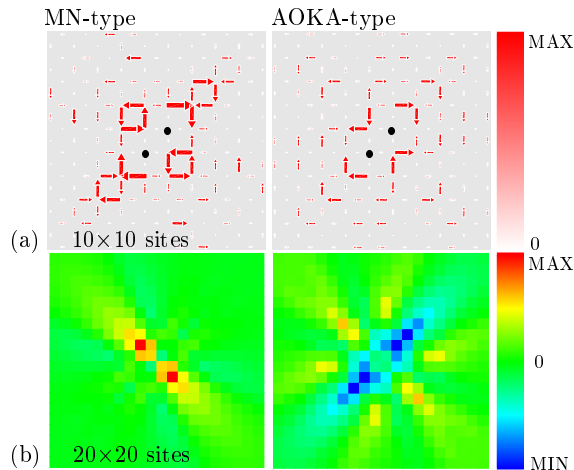


FIG. 4: (Color) The spontaneous current  $j_e(\mathbf{r})$  (a) and the internal magnetic field  $H(\mathbf{r})$  (b) for the MN-type (left panels) and the AOKA-type (right panels) pairings when a pair of impurities is situated in the diagonal direction. We show a region of  $10 \times 10$  sites for (a) and a region of  $20 \times 20$  sites for (b) around the impurities. Solid circles in (a) indicate the impurity sites.

direction perpendicular to the direction in which the impurities are aligned. The field orientation is toward the  $+z$  direction in this case. On the other hand, in AOKA-type pairing, the spontaneous field, oriented toward the  $-z$  direction, has strong intensity in the direction paral-

lel to the impurity alignment. This is a good example of phenomena in which a difference in the phase windings of the pairing function on the Fermi surface results in experimentally observable quantities.

In summary, we have calculated, on the basis of BdG equation, the spontaneous field and the electronic structure around the impurities in spin triplet chiral  $p$ -wave superconductor, where we compare the results between the MN-type pairing  $\sin p_x + i \sin p_y$  and the AOKA-type pairing  $\sin(p_x + p_y) + i \sin(-p_x + p_y)$ .

We have shown that differences between the two pairings appear in the LDOS structure at the sites nearest and next nearest to the impurity site. Namely, the zero energy LDOS at the nearest site is found to be larger (smaller) than the LDOS at the second nearest site for MN-type (AOKA-type) pairing. When a pair of impurities is situated in the diagonal direction, the spontaneous magnetic field distribution around the impurities is quite different between the two pairings. The spontaneous field has strong intensity along the line perpendicular (parallel) to the direction in which the two impurities are aligned in the MN-type (AOKA-type) pairing. We expect that the properties around the impurities shown here provide information for distinguishing the pairing state of  $\text{Sr}_2\text{RuO}_4$ .

The authors thank Y. Maeno, K. Ishida, H. Kontani, and Y. Yanase for valuable discussions. They also thank H. Aoki and R. Arita for stimulating discussions. This work was supported by a Grant-in-Aid for the 21st Century COE "Frontiers of Computational Science".

- 
- [1] Y. Maeno, H. Hashimoto, K. Yoshida, S. Nishizaki, T. Fujita, J.G. Bednorz, and F. Lichtenberg, *Nature* **372**, 532 (2002).
- [2] T. M. Rice and M. Sigrist, *J. Phys. Condens. Matter* **7**, L643 (1995).
- [3] K. Ishida, H. Mukada, Y. Kitaoka, K. Asayama, Z. Q. Mao, Y. Mori, and Y. Maeno, *Nature* **396**, 658 (1998).
- [4] J. A. Duffy, S. M. Hayden, Y. Maeno, Z. Q. Mao, J. Kulda, and G. J. McIntyre, *Phys. Rev. Lett.* **85**, 5412 (2000).
- [5] K. D. Nelson, Z. Q. Mao, Y. Maeno, and Y. Liu, *Science* **306**, 1151 (2004).
- [6] Y. Asano, Y. Tanaka, M. Sigrist, and S. Kashiwaya, *Phys. Rev. B* **67**, 184505 (2003); Y. Asano, Y. Tanaka, M. Sigrist, and S. Kashiwaya, *cond-mat/0502082*.
- [7] R. Jin, Y. Liu, Z. Mao, and Y. Maeno, *Europhys. Lett.* **51**, 341 (2000).
- [8] C. Honerkamp and M. Sigrist, *Prog. Theor. Phys.* **100**, 53 (1998).
- [9] M. Yamashiro, Y. Tanaka, and S. Kashiwaya, *J. Phys. Soc. Jpn.* **67**, 3364 (1998).
- [10] G.M. Luke, Y. Fudamoto, K.M. Kojima, M.I. Larkin, J. Merrin, B. Nachumi, Y.J. Uemura, Y. Maeno, Z.Q. Mao, Y. Mori, H. Nakamura, and M. Sigrist, *Nature* **394**, 558 (1998).
- [11] Y. Tanaka and S. Kashiwaya, *Phys. Rev. Lett.* **74**, 3451 (1995), S. Kashiwaya and Y. Tanaka, *Rep. Prog. Phys.* **63**, 1641 (2000), M. Yamashiro, Y. Tanaka, and S. Kashiwaya, *J. Phys. Soc. Jpn.* **67**, 3364 (1998).
- [12] Z. Q. Mao, K. D. Nelson, R. Jin, Y. Liu, and Y. Maeno, *Phys. Rev. Lett.* **87**, 037003 (2001); M. Kawamura, H. Yaguchi, N. Kikugawa, Y. Maeno, and H. Takayanagi, *J. Phys. Soc. Jpn.* **74** 531 (2005); F. Laube, G. Goll, H. v.Löhneysen, M. Fogelström, and F. Lichtenberg, *Phys. Rev. Lett.* **84**, 1595 (2000).
- [13] K. Miyake and O. Narikiyo, *Phys. Rev. Lett.* **83**, 1423 (1999).
- [14] T. Kuwabara and M. Ogata, *Phys. Rev. Lett.* **85**, 4586 (2000).
- [15] R. Arita, S. Onari, K. Kuroki, and H. Aoki, *Phys. Rev. Lett.* **92**, 247006 (2004).
- [16] T. Nomura and K. Yamada, *J. Phys. Soc. Jpn.* **69**, 3678 (2000).
- [17] Y. Yanase and M. Ogata, *J. Phys. Soc. Jpn.* **72**, 673 (2003).
- [18] K. Deguchi, Z.Q. Mao, H. Yaguchi, and Y. Maeno, *Phys. Rev. Lett.* **92**, 047002 (2004); K. Deguchi, Z.Q. Mao, and Y. Maeno, *J. Phys. Soc. Jpn.* **73**, 1313 (2004).
- [19] M. Takigawa, M. Ichioka, K. Machida, and M. Sigrist, *Phys. Rev. B* **65**, 014508 (2002).
- [20] C. Lupien, S.K. Dutta, B.I. Barker, Y. Maeno, and J.C.

- Davis, condmat/0503317.
- [21] M.I. Salkola, A.V. Balatsky, and J.R. Schrieffer, Phys. Rev. B **55**, 12648 (1997).
- [22] H. Tsuchiura, Y. Tanaka, M. Ogata, and S. Kashiwaya, Phys. Rev. Lett. **84**, 3165 (2000).
- [23] A.V. Balatsky, I. Vekhter, and Jian Xin Zhu. cond-mat/0411318.
- [24] Y. Okuno, J. Phys. Soc. Jpn. **69**, 858 (2000).